Heterosis for Biomass-Related Traits in Interspecific Triploid Hybrids of Willow (Salix Spp.)

Craig H. Carlson
Cornell University

Lawrence B. Smart (lbs33@cornell.edu)
Cornell University https://orcid.org/0000-0002-7812-7736

Research Article

Keywords: hybridization, hybrid vigor, polyploidy, short rotation coppice, woody plants, Salicaceae

Posted Date: April 8th, 2021

DOI: https://doi.org/10.21203/rs.3.rs-353369/v1

Version of Record: A version of this preprint was published at BioEnergy Research on July 7th, 2021. See the published version at https://doi.org/10.1007/s12155-021-10305-0.

Heterosis for Biomass-Related Traits in Interspecific Triploid Hybrids Of Willow (*Salix* Spp.)

Craig H. Carlson and Lawrence B. Smart[§]

Horticulture Section, School of Integrative Plant Science, Cornell University, Cornell AgriTech, Geneva, NY 14456 USA

[§]Corresponding Author:

Lawrence B. Smart

Address: 630 West North St., Geneva, NY, 14456

Email: lbs33@cornell.edu

Phone: 315-787-2490

Contact Information:

CHC: chc89@cornell.edu (ORCiD: 0000-0003-2050-5455)

LBS: lbs33@cornell.edu (ORCiD: 0000-0002-7812-7736)

Running Title: Heterosis in triploid willow

Abstract

Species hybridization is key for the improvement of shrub willow (*Salix* spp.) bioenergy crops, because hybrids often display heterosis for yield. Development of high-yielding genotypes requires numerous broad attempts at hybridization followed by field evaluation and selection for stable performance. Selection of improved shrub willow varieties for use as a bioenergy crop involves evaluation of full-sib progeny in family-based selection trials. Improving the accuracy of evaluation would greatly improve the efficiency of selection. Heterosis for biomass yield in intra- and interspecific F_1 and F_2 shrub willow (*Salix* spp.) was examined utilizing a suite of biomass, foliar, and physiological traits collected over the course of 12 weeks in the greenhouse and over two years in the field. Triploid families generated from diploid *S. viminalis* and tetraploid *S. miyabeana* displayed the greatest levels of heterosis for harvestable biomass and

biomass-related growth traits in the greenhouse and in the field. While intraspecific *S. purpurea* diploids exhibited low levels of heterosis for these traits, interspecific diploids produced moderate levels of heterosis in greenhouse experiments. Differences between greenhouse and field trial results can largely be explained by pest damage, which negatively impacted interspecific diploids. Heterosis for the traits that form the basis for biomass yield, including stem growth, foliar, and physiological traits, was quantified and family-level differences are discussed.

Key Words: hybridization, hybrid vigor, polyploidy, short rotation coppice, woody plants, Salicaceae

Word count: 5808 words

Introduction

Shrub willows (*Salix* spp., Salicaceae) are vigorous woody perennials that can be harvested to provide feedstocks for biofuel and bioenergy production [1]. Commonly found as pioneer species and in riparian habitats, the range of *Salix* extends from the arctic plains to the subtropics, with more than 350 species have been described [2,3]. *Salix* spp. are dioecious outcrossing perennials that are mostly entomophilous with possible low proportions of anemophily [4,5]. As *Salix* is particularly amenable to wide-hybridization, taxonomic characterization within the genus has been an enduring challenge for botanists and breeders alike [6]. In sympatric populations of *Salix*, members within the same section will often hybridize, which can generate mixed populations of both pure species and species hybrids [7]. In addition, vegetative clonal propagation can be a significant contributor to population structure in *Salix*, and has been shown to be fairly common in naturalized stands of North American *S. purpurea* [8]. Beyond the tremendous ecological amplitude, the heterogeneity and adaptive plasticity of *Salix* delivers a prodigious source of germplasm for genetic improvement.

Modern domestication of *Salix* traces back to the Swedish geneticist Nils Heribert-Nilsson's early cytological studies of *S. viminalis* × *S. caprea* hybrids in the 1920's [9]. Shortly thereafter, willow conservation and breeding was principally led by H.P. Hutchinson and K.G. Scott for nearly 30 years at the Long Ashton Experiment Station in the UK. Since the 1970's, breeders have maintained a goal of producing fast-growing shrub willow bioenergy feedstock cultivars that are high-yielding, genetically diverse, resistant to pests and diseases, and amenable to marginal sites, without competing with food crops [10]. A thorough review of willow botany and breeding can be found in [11].

While most complex quantitative traits, including yield, generally display additive inheritance, deviations from the midparent value in the F_1 can result in either hybrid vigor or hybrid necrosis [12]. Since the Green Revolution, the phenomenon of hybrid vigor (heterosis) has been exploited in crop systems, more than doubling global commodity yields in only a few decades. Plants expressing heterosis are thought to have experienced one or more duplication events in their past [13] and many crop plants are polyploid. There is no unifying model to predict heterosis in interspecific hybrid plants, while much of the body of literature has been centered on the comparison of hybrids generated from inbred or synthetic allopolyploids. Common in *Salix*,

71 polyploidy is thought to be largely due to allopolyploidization events [14]. Polyploidy via
72 chromosome doubling or wide hybridization can have a positive impact on the accumulation of
73 biomass in hybrids, compared to progenitors [15]. In most plant crops, aneuploidy generally
74 corresponds with hybrid necrosis due to the negative impact of sub-optimal gene dosages on
75 protein function and metabolic homeostasis [12].

76 In order to advance the adaptive capacity of the US agricultural and energy sectors to respond to
77 climate change, plant breeders must develop regionally adapted and sustainable bioenergy crops
78 displaying hybrid vigor. Shrub willow has emerged as a highly sustainable bioenergy feedstock
79 that can directly substitute for fossil fuels with great potential for yield increases through species
80 hybridization. Through careful hybridization, phenotypic evaluation, and selection, substantial
81 improvements have been made in shrub willow biomass yield [16] and lignocellulosic
82 composition (quality) [17]. Species hybridization is a key component in the development of
83 shrub willow bioenergy crops, as hybrids often display heterosis for yield [18]. Interspecific
84 hybridization is also thought to be important in the generation of diverse secondary metabolites,
85 and that selection may favor plants expressing novel profiles [19]. For instance, interspecific
86 shrub willow populations have been implicated in enhanced resistance to pests [20,21] and
87 pathogens [22], and has been attributed to differential expression of metabolites [23,24],
88 resistance genes [21], as well as overall increased vigor [25].

89 Although heterosis has been observed in intraspecific crosses [26], it is more pronounced in
90 triploids derived from the hybridization of diploid and tetraploid parents [27]. Ever since
91 Nilsson-Ehle (1936) first reported finding naturally occurring “gigas” triploid *Populus tremula*
92 L. in the forests of Sweden [28], polyploids have garnered substantial interest in tree breeding
93 and research. Previous shrub willow yield trials have shown that elite triploid hybrid cultivars
94 produce greater biomass yield compared to diploids and exceed or are not significantly different
95 from tetraploids [29]. In addition, there is evidence that triploids have the potential to produce
96 more cellulose per unit area because of higher biomass yields and/or cellulose content [17].
97 However, little is known about the genetic mechanisms responsible for heterosis in triploid
98 willow [30] because there has been no systematic survey of heterosis from triploids.

99 The inherent time and investment associated with cultivar development in woody perennial
100 feedstocks require efficient population development and phenotypic evaluation methods to

significantly increase gains in biomass yield. Evaluation of large populations of progeny will be necessary to make significant gains, which requires early screening to reduce the costs associated with long-term field trials. The families referenced in this study were generated from crosses made between parents of differing ploidy and taxonomic section within the genus *Salix*, involving diploid *S. purpurea* and tetraploid *S. miyabeana* in the Sect. Helix Dumont, and diploid *S. viminalis* in the Sect. Vimen (formerly Viminella Seringe). The main objectives of this study were (1) to compare and contrast extensive phenotypic data collected among eight intra- and interspecific shrub willow families, (2) to determine the extent to which these families display heterosis for biomass-related traits and biomass yield, and (3) determine if there is concordance of heterosis when plants are grown in the greenhouse compared with the field.

Materials and Methods

Population Development

A total of eight full-sib F_1 and F_2 families were generated from crosses between diploid and tetraploid parents representing three *Salix* species: *S. purpurea* Sect. Helix (2n=2*x*=38), *S. viminalis* Sect. Vimen (2n=2x=38), and *S. miyabeana* Sect. Helix (2n=4*x*=76). The full-sib F_1 *S. purpurea* family 82 was generated from a cross between female 94006 and male 94001, both collected from naturalized *S. purpurea* populations in upstate NY. Two F_1 offspring from this cross, female *S. purpurea* 'Wolcott' (9882-41) and male *S. purpurea* 'Fish Creek' (9882-34), were crossed to generate the full-sib F_2 *S. purpurea* family 317. The female *S. purpurea* genotype 94006 was crossed with the male *S. viminalis* 'Jorr' to generate the interspecific diploid family 407, and a cross between *S. viminalis* 07-MBG-5027 and the male *S. purpurea* genotype 94001 generated the 'pseudo-reciprocal' interspecific family 421. Female diploid genotypes 94006 and 07-MBG-5027 were separately crossed with tetraploid *S. miyabeana* male 01-200-003, to generate the interspecific triploid families 415 and 423, respectively. Triploid family 430 was generated from a cross between the tetraploid *S. miyabeana* female 01-200-006 and diploid *S. viminalis* male 'Jorr'. Finally, the intraspecific *S. miyabeana* tetraploid family 425 resulted from a cross between female 01-200-006 and male 'SX64'. All family progeny individuals and their parents were planted in nursery beds at Cornell AgriTech (Geneva, NY).

Greenhouse Design

Parent genotypes and randomly chosen progeny from the eight families described above were grown from stem cuttings (20 cm) in 12-L plastic pots with peat moss-based potting mix (Fafard, Agawam, MA) to evaluate growth traits under greenhouse conditions over the course of 12 weeks. Families consisted of 12 progeny individuals and their parents, for a total of 104 genotypes (Table 1). One exception is that the male parent 'SX64' of the intraspecific *S. miyabeana* family 425 was not included. Plot was defined as a single cutting planted in a pot, which were arranged in a randomized complete block design with four replicate blocks. Two blocks were located on benches in one greenhouse with the other two blocks in an adjacent greenhouse set for identical growing conditions. Supplemental greenhouse lighting was provided on a 14-h day : 10-h night regimen with max daytime temperature of 26°C and a nighttime temperature of 18°C. Liquid fertilizer (Peter's 15-16-17 Peat-Lite Special®, Scott's, Marysville, OH) was applied weekly after week four according to manufacturer recommendations.

Field Design

The field trial was established at Cornell AgriTech (Geneva, NY) in a randomized complete block design with four replicate blocks of three-plant plots. To avoid edge effects, *S. purpurea* parent genotypes 'Fish Creek' and 94006 were planted as border rows along the east and west sides of the trial, respectively, and the north and south ends were buffered by a single row of genotype 94006. Within-row spacing was 0.4 m and spacing between rows was 1.82 m. The soil at the field site is Odessa silt loam with a depth to water table of 25 to 45 cm. For additional site characteristics, see [30,31].

Determination of Ploidy Level

The relative DNA content (2C-value in pg) of family parents and progeny was determined by flow cytometric analysis using young leaf material harvested from actively growing shoots in greenhouse conditions. Analysis of 50 mg of mature leaf tissue from parental genotypes and selected progeny was performed at the Flow Cytometry and Imaging Core Laboratory at Virginia Mason Research Center in Seattle, WA. A minimum of four replicates of all samples were independently assessed using either the diploid *S. purpurea* female genotype 94006 or the diploid *S. purpurea* male genotype 94001, and the tetraploid *S. miyabeana* female genotype 01-200-006 or the tetraploid *S. miyabeana* male genotype 01-200-003 as internal standards. Diploid and tetraploid parent genotypes from multiple runs were averaged and then divided by the value

of the check for that run. This factor was then multiplied by each sample value within the same run as the check. When a genotype was analyzed more than once, the pg $2C^{-1}$ values were averaged.

Greenhouse Phenotypes

Starting approximately 7 d after planting (dap), the vegetative phenology stage (PHE) of each plot was scored at 7, 9, 11, 13, and 15 dap. Vegetative phenology was scored as six stages described as: stage (0) dormant axillary buds are tightly closed and covered by bud scales; (1) axillary buds begin to swell and change color; (2) generative bud burst with visible leaves; (3) leaves emerge and begin to unfold; (4) unfolded leaves begin expanding; and (5) at least two leaves are fully expanded. To provide an indirect measurement of leaf chlorophyll and nitrogen content, leaf color was measured using a Minolta SPAD 502 Chlorophyll Meter (Spectrum Technologies, Inc., Aurora, IL). Four fully-expanded leaves sampled from the upper 25% of the canopy were measured and averaged for each plant at 14, 42, and 70 dap. Sex of progeny individuals was determined by visual observation after forcing 2-3 dormant shoots to flower in greenhouse conditions an d was confirmed in field trial plots.

Primary stems were defined as those emerging from dormant axillary buds and ≥6 cm in length. Secondary stems were defined as emerging from axillary buds on the primary stem from current-season growth (sylleptic) and were counted as the total number of secondary branches within each plot with a PHE ≥3. The length of each stem per plant was measured from the proximal base of the primary stem to the distal inner-whorl of the leaf primordia. The sum of stem lengths for each plot was considered to be the total stem length (TSL) and mean stem length (MSL) per plant was the mean of individual stem lengths. Starting 14 dap to 70 dap, all primary stems were measured within each plot once a week, totaling nine measurement time points.

The diameter of each primary stem within a plot (SDIA) was measured at the base the final week of the study using a digital caliper. Stem diameter measurements were used to calculate the area (SA) of all stems >20 cm in length. Sum of stem area per plant (SSA) was calculated by summing individual SA per plant. An estimate of total stem volume (VOL) was modeled as a cone by multiplying SSA times 1/3 plot height.

In order to predict root biomass (RDW), root electrical capacitance (REC, nF) was measured according to the protocol described in [32]. Root biomass was harvested from a subset of 20 pots (2-3 progeny individuals per family) that were selected from the 416 pots as representing a distribution of capacitance readings, ranging from 70.5 to 283.8 nF. To assure the retrieval of fine root hairs, potting mix was washed from roots by first soaking root balls in water for 12 h without their pots then rinsing them by hand repeatedly and decanting into 2.4 mm and 1.0 mm aluminum test sieves. Root samples were considered appropriate for dry weight analysis when root biomass was visually free of debris. Root biomass and cuttings were separately dried in an oven and weighed.

Leaf area (LFA) was determined using a portable leaf area meter (Model No. CI-203, CID Inc., Camas, WA). A representative leaf from each plot was scanned, then excised, dried to constant weight at 65°C, and weighed to obtain leaf dry weight (LFDW). Leaf petioles were excluded from LFA and LFDW measurements. Specific leaf area (SLA) was calculated as the ratio of the total leaf area (cm^2) and dry weight (g). Leaf aspect ratio (LFR) is the ratio of the leaf length to its maximum width. Leaf shape factor (LFF) or the ratio of leaf area to the leaf perimeter, was corrected so that the shape factor of a circle is equal to one: $4\pi(LFA/LFP^2)$. Stem and leaf biomass was harvested separately from each plot, dried in an oven to constant weight at 65°C, then weighed to determine total stem dry weight (SDW) and total leaf dry weight (LDW).

Field Phenotypes

During the dormant period after each growing season, DIA of stems ≥5 mm were measured at 30 cm from the base of the plant using Masser Racal 500 digital caliper (Masser, Rovaniemi, Finland) and stem number was counted for each plant. The SA of each stem was calculated from DIA and SSA per plant was calculated by summing the areas of every stem. Maximum stem height (HT) of every plot was recorded using a measuring rod (Crain Enterprises, Inc., Mound City, IL).

Physical and chemical wood properties were measured for four replicates. Stem segment samples were collected in the dormant period after each growing season using sampling methods previously described (Liu et al., 2015) and were stored frozen at -4°C until they were processed. The specific gravity of each sample was measured by volumetric displacement (TST om-06, 2006). In 2014, a modified method of measuring specific gravity was used where the volume of

water displaced was weighed for added precision. Following specific gravity determination, stem segments were oven-dried at 65°C to a constant weight and then rough milled to a 5 mm particle size with a Retch SM300 cutting mill (Retch, Haa, Germany) and were further comminuted to <0.5 mm particle size by fine milling with the IKA MF 10.1 knife mill (IKA, Wilmington, NC) for compositional analysis. Approximately 20 mg of each milled stem sample was analyzed with a Thermogravimetric Analyzer (TGA) Q500 instrument and Universal Analysis 2000 version 4.5A software (TA Instruments, New Castle, DE), as previously described (Serapiglia et al., 2009). Hemicellulose, cellulose, lignin, and ash content were determined as a percentage of total dry biomass for each sample, as previously described in [30].

At the end of the second growing season, crown diameter (CDIA) was measured using modified Haglöf Mantax forestry calipers (Haglöf Sweden AB, Långsele, Sweden). Stool diameters were measured at 15.24 cm above the soil, which is the average height of a shrub willow harvester. Crown form (FORM) was calculated by multiplying the *arctangent2* of one-half CDIA and the fixed distance at which CDIA was measured (15.24 cm) by 180/π, to obtain the angle of the stem branching relative to the soil.

Statistical Analysis

All statistical analyses and plotting were performed within the open-source statistical computing environment, R [33]. For quantitative traits listed in Table 2, a Shapiro-Wilk test was conducted to detect a significant departure from normality. For non-normal data, the *boxcox* function was used to maximize the Shapiro-Wilk W statistic by computing log-likelihoods for the parameter (λ) of the Box-Cox power transformation, such that either a single-parameter $(y^{\lambda} - 1)/\lambda$ or two-parameter $[(y - \lambda_2)^{\lambda_1} - 1]/\lambda_1$ power transformation was applied. For repeated measurements of quantitative traits HT, MSL, and TSL, growth rates were determined using Gompertz 3-parameter function: $ce^{-e^{-a(t-b)}}$, whereas ordinal PHE and PSN growth rates were determined using the following 3-parameter logistic function: $c/(1 + e^{-a(t-b)})$, where, a is the growth rate, b is the inflection point, c is the asymptote, and t is time (in dap).

Tests for association between binary and quantitative traits were done using Pearson's product moment correlation coefficient (r) at a confidence level of 95%. Correlations between ordinal and quantitative or binary trait pairs were tested using Spearman's rank correlation coefficient,

whereas Kendall's rank correlation was used to test ordinal trait pairs. To correct for multiple comparisons, a Bonferroni correction was applied by multiplying *P*-values by the number of pairwise comparisons. Genotypes were divided based on ploidy, sex, and pedigree. A Wilcoxon Rank Sum test was used to test whether two sample distributions differ. When significant differences were observed, treatment comparisons were performed using Tukey's Range test.

Variance components for the greenhouse trial were estimated with *lmer* in the package lme4 [34] using the Restricted Maximum Likelihood (REML) method, for the following model:

$$y_{ij} = \mu + \alpha_i + \beta_j + \varepsilon_{ijk}$$

where y_{ijk} is the observed value, μ is the overall mean, α_i is the effect of genotype i, β_j is the effect of block j, and ε_{ijk} is the random error, which is assumed independent and identically distributed.

Field trial dimensions were 388.6 m × 36.6 m (Supplementary Fig. S1), which introduced spatial variation not easily accountable by block alone. Thus, to account for spatial variation in the field trial, following the approach outlined in [35], spatial trends (row and column) in the field trial were modeled as two-dimensional Penalized (P)-splines, using *SpATS* and *SAP* functions (n.seg = (16, 64), tolerance = 1×10^{-6}) in the SpATS package [36]. The conditional means of random effects were extracted from the above linear mixed model in order to provide the relative phenotypic contributions of the male and female parents. Midparent heterosis (MPH) was calculated as the percent deviation of the F_1 progeny mean relative to the geometric mean of the parents. In this case, genotype (clone) was fixed in the linear model, so MPH represents deviations from these estimates. Fisher's Exact test was used to classify phenotypic expression into modes of inheritance ($P < 0.05$) by comparing the deviation of the F_1 to each parent. For the reason that the male parent of the intraspecific tetraploid F_1 *S. miyabeana* family 425, cv. 'SX64', was not present, only the deviation of the F_1 from the female parent 01-200-006 was reported.

Results and Discussion

Harvestable Biomass in the Greenhouse Trial

Of the 104 genotypes harvested in this trial, total aboveground biomass (AGB, g) ranged from 119.6 g to 51.1 g (Fig. 1). The greatest yielding genotype was a triploid hybrid, *S. viminalis* × *S. miyabeana* 12X-423-043, and the least yielding genotype was a diploid *S. purpurea*, 10X-082-078. The greatest mean AGB was from the *S. viminalis* × *S. miyabeana* triploid family 423 (100.3 ±3.8) and the *S. miyabeana* × *S. viminalis* triploid family 430 (98.7 ±3.4), followed by the *S. viminalis* × *S. purpurea* diploid family 421 (92.3 ±3.8). All other families were not significantly different from one another, with a family mean AGB ranging from 78.9 to 82.5 g.

The mean AGB of triploids (93.8 ±1.6) was significantly greater (Wilcoxon $P < 0.001$) than the mean AGB of diploids (82.6 ±1.3) and tetraploids (79.8 ±2.6). While the triploid families 423 and 430 did show greater AGB than both diploid and tetraploid parents, AGB did not exceed the midparent for the triploid family 415 (Fig. 2). Similarly, belowground dry biomass (RDW, g), which was estimated using the REC method described in [32], ranged from 11.1 g to 42.5 g, with the triploid family 430 had accumulating the greatest RDW, followed by families 423 and 421, with the lowest mean family REC values from the *S. purpurea* × *S. miyabeana* family 415. The mean RDW of triploids (26.6 ±0.8) was significantly greater (Wilcoxon $P < 0.001$) than that of diploids (23.1 ±0.6) and tetraploids (22.2 ±0.9), with no significant difference between diploids and tetraploids (Wilcoxon $P = 0.57$) (Fig. 1c).

Biomass ratios LDW SDW^{-1} and RDW SDW^{-1} for tetraploid genotypes were significantly greater than those of triploids and diploids (Wilcoxon $P < 0.001$), whereas diploids had significantly lower LDW SDW^{-1} and RDW SDW^{-1} ratios compared to both triploids and tetraploids (Wilcoxon $P < 0.001$) (Fig. 1d). The tetraploid *S. miyabeana* family 425 had the greatest LDW SDW^{-1} ratio (0.76 ±0.02) and the triploid *S. miyabeana* × *S. viminalis* triploid family 430 had the greatest RDW SDW^{-1} ratio (0.53 ±0.02). Further, the diploid F_2 *S. purpurea* family 317 had the lowest LDW SDW^{-1} ratio (0.50 ±0.01) and the triploid *S. purpurea* × *S. miyabeana* family 415 had the lowest RDW SDW^{-1} ratio (0.38 ±0.02), yet was not significantly different from both intraspecific F_1 and F_2 *S. purpurea* families. Subsequently, the ratio of SDW to the total biomass (TBM) showed the converse, which suggests that diploids placed considerably less energy into leaf biomass production (28.9 ±0.4) compared to triploids (36.6 ±0.6, Wilcoxon $P < 0.001$) and tetraploids (34.4 ±1.4, Wilcoxon $P < 0.001$).

Biomass-Related Stem Growth in the Greenhouse

Growth measurements taken at the end of the study included the length and diameter of every stem, as well as primary and axial stem number. The greatest plot HT after 84 dap in the greenhouse was observed for the triploid hybrid, *S. viminalis* × *S. miyabeana* 12X-423-034 (2.1 ±0.05), whereas the genotype with the lowest HT was the intraspecific tetraploid, *S. miyabeana* 12X-425-106 (1.2 ±0.09). Total stem length (TSL) was calculated as the sum of the length of each shoot >20 cm per plot, and ranged from 6.03 m to 1.95 m. While TSL of diploids (3.89 ±0.08) and triploids (3.88 ±0.10) was not significantly different (Wilcoxon $P = 0.85$) at 84 dap, tetraploids showed significantly less TSL (3.47 ±0.13) than diploids (Wilcoxon $P = 0.02$) and triploids (Wilcoxon $P = 0.01$). The lower TSL values for tetraploids may be explained by lower PSN and ASN after 84 dap, thus leading to fewer stems and lower TSL than diploids and triploids. Although triploids had a greater MSL (1.62 ±0.02) at 84 dap (Wilcoxon $P < 0.001$), diploids (1.44 ±0.02) and tetraploids (1.49 ±0.04) were not significantly different (Wilcoxon $P = 0.11$). The sum of DIA sampled were used to calculate MDIA and sum stem area (SSA) for each plot. The MSA ranged from 0.37 to 1.41 cm^2 and SSA ranged from 1.29 to 2.95 cm^3.

Sex Ratio Bias

While the selection of individuals for each family was completely random, all families had a greater proportion of female progeny, of which five of the eight families were sex-biased (χ^2 $P < 0.05$) (Table 1). Female to male sex ratios ranged from 1.13 to 4.56. Notably, the triploid *S. miyabeana* × *S. viminalis* family 430 was all-female. Sex ratio bias is not uncommon in willows (primarily female-biased) [37-43], but infrequently found in poplars (primarily male-biased) [44]. Whether influenced by environmental factors, unique mechanisms of sex determination, or sex chromosome dosage, the genetic basis of biased sex-ratios in *Salix* reported here and elsewhere are not known.

Foliar and Physiological Traits

Vegetative phenology recorded at 7, 9, 11, and 13 dap demonstrate significantly faster budbreak, leaf expansion, and early shoot development in triploids, compared with diploids and tetraploids (Fig. 3a). Diploids, while significantly lagging triploids and tetraploids early on, were not significantly different from tetraploids by 13 dap. For each plot, three SPAD readings were taken at 14, 42, and 70 dap to assess the chlorophyll content or nitrogen status of fully-expanded leaves from the upper 30 cm of the canopy. A significant interaction was identified for SPAD by time

and ploidy as well as time and family. While the initial SPAD reading at 14 dap showed marginally greater values for triploids and tetraploids, the opposite trend was found for later readings (Fig. 3b). Diploid genotypes showed significantly greater SPAD readings at 42 dap than triploids and tetraploids, which were not significantly different. By 70 dap, differences in SPAD readings by ploidy were not as great as those taken at 42 dap. This was also observed for SPAD readings taken in the field trial, where higher ploidy was inversely correlated with greater SPAD readings.

Leaf measurements obtained at 11 weeks included leaf area (LFA), length (LFL), width (LFW), perimeter (LFP), ratio (LFR), and dry weight (LFDW). Of all the genotypes in the trial, the intraspecific tetraploid, *S. miyabeana* 13X-425-110, had the greatest LFA (40.0 ±7.5), whereas the diploid hybrid, *S. purpurea* × *S. viminalis* 11X-407-087, had the smallest LFA (8.9 ±1.6). On a family-level, the intraspecific *S. miyabeana* family 425 had the greatest LFA (22.0 ±1.2) and the intraspecific F_1 *S. purpurea* family 82 had the smallest LFA (13.9 ±0.5). Mean LFL ranged from 17.5 cm to 6.6 cm. Among the top 50th percentile for the leaf dimensions LFA, LFL, and LFW, nearly all genotypes had either the *S. viminalis* female 07-MBG-5027 or the *S. viminalis* male 'Jorr' as a parent.

Given that all plots received the same fertilizer and application rate, it may be that the nitrogen status of leaves is concentrated to less leaf area in diploids, given the significantly greater SPAD values in diploids, compared with those of triploids and tetraploids. Further, LFA and LDW of triploid F_1 individuals showed primarily additive inheritance, and on the basis of ploidy, triploids were intermediate to diploids and tetraploids for the same traits. Yet, under controlled environmental conditions, higher ploidy tended to result in greater leaf area and biomass, but a lower leaf nitrogen status. One possible explanation for this is that polyploid willows are more efficient in the production of *low resource* leaves [45]; perhaps by focusing available nutrient resources to a rapidly emerging canopy, rather than uniformly along the stem, as is likely the case in diploids. Triploid genotypes with an intermediate LDW SDW^{-1} ratio could indicate more efficient partitioning of photoassimilate from leaves to sink organs. While this attribute would surely stimulate the rapid accumulation of biomass, diploids could benefit in nutrient-scarce environments by sustaining growth rates, whereas higher ploidy levels would likely show an overall reduction in their growth rate.

364 *Multivariate Analysis*

365 Traits that were non-informative in biomass yield predictions, but correlated with informative
366 predictors, may still prove to be of relative importance, particularly when assayed in additional
367 environments or pedigrees. While many of the traits listed in Table 2 were strongly correlated
368 with those important for biomass yield, some pairs tended to be more autocorrelated
369 (Supplementary Fig. S3), as they were repeated measurements or components of the same trait.
370 The greenhouse-collected traits showing the highest correlations with SDW were VOL (r =
371 0.73), REC (r = 0.78), and LDW (r = 0.62); all grouping closely. Following these traits, later
372 stem length measurements were most correlated to SDW, whereas, PHE at 11 and 13 dap and
373 ASN at 56 dap were most correlated with LDW. Although weakly, both SDW and LDW had
374 inverse relationships with the inflection point of HT.

375 Phenological stages (PHE) recorded at 11 and 13 dap in the greenhouse were strongly correlated
376 with SPAD at 14 dap, LFR, LFL, TSL at 14 and 21 dap, and the growth rates of HT, MSL, TSL,
377 but not STN. Early PHE measurements at 7 and 9 dap were positively correlated with CVAL and
378 LFR. At 13 and 15 dap, PHE was only weakly correlated with SPAD at 42 dap. All PHE
379 measurements were inversely correlated with LFW, SLA, and the ratio STN AGB^{-1}. Leaf
380 dimensions LFL, LFA, and LFP, as well as the biomass ratio LDW SDW^{-1} were strongly and
381 positively correlated ($r > 0.5$) with CVAL, whereas both SPAD at 42 dap and SLA were
382 inversely correlated ($r < -0.5$). Besides showing positive correlations to the ratios SDW TOT^{-1}
383 and STN AGB^{-1}, SLA was the solitary trait to be inversely correlated with nearly all growth
384 traits. Along with SLA, SDW TOT^{-1} and STN AGB^{-1} were most negatively correlated with leaf
385 dimensions, as well as SPAD at 42 dap and STN measurements. Root electrical capacitance
386 (REC), SSA, TSL at 28 dap, and PHE at 11 and 13 dap were highly correlated with SDW, and
387 have been shown to account for a large proportion of the variance (R^2 = 0.69) in multiple linear
388 regression [32].

389 Repeated measures have commonly been used to identify growth patterns in response to
390 environmental factors or treatments. Here, the treatments under consideration were pedigree and
391 ploidy level. While the inherent differences between factors tend to inflate the actual differences
392 (e.g., diploids versus tetraploids), relative growth rates (RGR) act as a standardized measure of
393 growth and offer more impartial comparisons. Early vegetative PHE measurements showed that

394 triploids are faster to break bud and grow at faster rates compared with diploids and tetraploids.
395 However, over time, diploids maintained more linear growth rates compared with those of
396 triploids, which leveled-off approximately 8 weeks after planting. This could be due to
397 increasingly limited space in the pots of triploids, as they exhibited both greater above and
398 below-ground biomass at the termination of the study, especially for individuals with *S. viminalis*
399 as one of the parents, as described in [32]. It may be that *S. viminalis* crosses have a higher
400 propensity for accumulating root mass than intraspecific or interspecific crosses of *S. purpurea*
401 and *S. miyabeana*. Using the REC phenotyping method, genetic mapping of this trait could
402 improve our understanding of root development and response to drought among willow crosses.
403 Marker-assisted selection (MAS) for REC could subsequently be used to improve biomass yield,
404 in the case that field evaluations correlate well with those in the greenhouse.

405 For field-collected biomass traits, all were highly correlated across years (Supplementary Fig.
406 S4). However, foliar traits were positively, but more weakly correlated between years, besides
407 leaf ratio (LFR) ($r = 0.65$, $p < 0.001$) and leaf shape factor (LFF) ($r = 0.35$, $p < 0.001$). Crown
408 form (FORM) measurements for all three years measured were most inversely correlated with
409 biomass stem growth traits (e.g., SA, HT, VOL, and STN) as well as wood density (DEN).
410 Wood chemical composition traits were also highly correlated, whereby LIG and ASH were
411 inversely correlated with CLS and HCL. Wood density (DEN) was only positively correlated
412 with CLS, but inversely correlated with HCL and ASH. Overall, individuals with higher ploidy
413 levels tended to have greater ASH and lower HCL, compared with diploids (Supplementary Fig.
414 S5).

415 *Concordance of Heterosis for Common Greenhouse and Field Traits*

416 Field-collected traits for the same families resulted in similar levels of heterosis for common
417 traits collected in the greenhouse trial (Fig. 4, Fig. 6). For instance, families 423 and 430 showed
418 the greatest MPH for HT, SA, and VOL for both years in the field trial as well as in the
419 greenhouse trial. While the interspecific diploid families 407 and 421 showed marginal levels of
420 MPH for the same traits, it was not observed in the field trial as a result of a high-incidence of
421 potato leafhopper and Japanese beetle feeding on individuals with a *S. viminalis* background,
422 also described in [21]. Yet, this was not observed for triploid families with a diploid *S. viminalis*
423 parent, which suggests some level of resistance in the hybrids.

Of the two years in the field trial, foliar traits were shown to be the most variable between years (Fig. 6, Supplementary Fig. S6). This was due to differences in precipitation during the 2015 and 2016 growing seasons. In 2015 growing conditions were nearly optimal throughout the season, but 2016 suffered a long stretch of mid-summer drought. Although individuals did not dramatically differ in MPH for most trait rankings between growing seasons, foliar trait MPH variation can be assessed by SLA. However, families 421, 423, and 430, which all had a *S. viminalis* parent, did show greater MPH for foliar traits in both the greenhouse and field trials. Remarkably, triploid individuals, 12X-423-060 and 12X-423-110, had average LFL >40 cm, which was nearly two-fold greater than the better parent.

Midparent Heterosis and Patterns of Inheritance

Our data show that relative to diploid and tetraploid genotypes triploids exhibit greater levels of heterosis for biomass yield and correlated growth traits, especially for crosses made between *Salix* Sections (Fig. 4, Supplementary Fig. S2). The interspecific diploid family 421 and interspecific triploid families 423 and 430 have *S. viminalis* as one of the parents, and all showed high levels of MPH (%) for total SDW and RDW, as well as RGR and early TSL and PHE measurements. However, MPH for total biomass or stem growth measurements were not observed in interspecific *S. purpurea* × *S. viminalis* family 407 or the intraspecific *S. purpurea* or *S. miyabeana* F_1 families.

The $\log_2$ difference of the respective female and male parent from the family progeny was determined in order to assess global inheritance patterns for all biomass-related traits in each family (Fig. 5). The diploid F_2 *S. purpurea* family 317 showed the most conserved inheritance for all traits, whereas the diploid F_1 *S. purpurea* family 82 showed greater levels of both P1- and P2-dominant as well as underdominant inheritance. The reciprocal interspecific diploid families 407 and 421 showed strong patterns of dominance, almost exclusively in the direction of the *S. viminalis* parent species. While stem traits for the triploid *S. purpurea* × *S. miyabeana* family 415 primarily displayed P2-dominant inheritance, foliar traits within the family reflected more conserved or additive inheritance. The triploid *S. viminalis* × *S. miyabeana* family 423 showed strong P1-dominant inheritance for all traits, comparable to the diploid *S. viminalis* × *S. purpurea* family 421. Although many traits in family 423 showed P1-dominant inheritance, conserved or additive inheritance for foliar traits were predominant, compared to that of stem traits in the same

454 family. Unlike triploid family 423, the triploid *S. miyabeana* × *S. viminalis* family 430 had the
455 greatest number of transgressive traits compared to all other families and showed nearly equal
456 P1- and P2-dominant inheritance patterns.

457 The heterozygous nature of *Salix* prevents a genetically uniform F_1 and both hybrid vigor and
458 hybrid necrosis can be represented by siblings of the same cross. Here, we demonstrate that
459 triploid shrub willow hybrids, derived from diploid and tetraploid parents of different species,
460 exhibit both dominant and transgressive phenotypic expression. Most notably, this was observed
461 for biomass growth traits for crosses between *Salix* Sections *Helix* and *Vetrix*.

462 **Conclusion**

463 The results outlined here corroborate consistent findings that triploids produce greater biomass
464 yields than their diploid or tetraploid parents. Heterosis for many of the extensive traits collected
465 in the greenhouse also showed heterosis in the field, with consistently greater total stem volume
466 among triploid individuals. The genetic basis of heterosis in willows is not well understood, and
467 further work on characterizing this phenomenon will support community efforts in build a toolkit
468 for improving this sustainable, fast-growing bioenergy crop.

469 **Declarations:**

470 *Funding:* This research was supported by the U.S. Department of Energy, Office of Science,
471 Office of Biological and Environmental Research (grant no. DE-SC0008375) and US
472 Department of Agriculture National Institute for Food and Agriculture (grant no. 2018-68005-
473 27925).

474 *Conflicts of Interest:* The authors declare that they have no conflicts of interest.

475 *Availability of data and material:* All data not presented in the paper or supplementary material
476 will be made available upon reasonable request to the corresponding author.

Acknowledgements: We are grateful to Smart Lab members Curt Carter, Lauren Carlson, and Dawn Fishback for their excellent technical assistance, and to Fred Gouker and Eric Fabio for assistance with harvesting and processing plants.

References

1. Smart LB, Cameron KD (2012) Shrub Willow. In: Kole C, Joshi CP, Shonnard DR (eds) Handbook of Bioenergy Crop Plants. CRC Press, Boca Raton, FL, pp 687-708. https://doi.org/10.1201/b11711-32

2. Lauron-Moreau A, Pitre FE, Argus GW, Labrecque M, Brouillet L (2015) Phylogenetic relationships of American willows (*Salix* L., Salicaceae). PLoS ONE 10:e0121965. https://doi.org/10.1371/journal.pone.0121965

3. Argus GW (1997) Infrageneric classification of *Salix* (*Salicaceae*) in the New World. Syst Bot Monogr 52:1-121.

4. Argus GW (1974) An experimental study of hybridization and pollination in *Salix* (willow). Can J Bot 52:1613-1619. https://doi.org/10.1139/b74-212

5. Tamura S, Kudo G (2000) Wind pollination and insect pollination of two temperate willow species, *Salix miyabeana* and *Salix sachalinensis*. Plant Ecol 147:185-192. https://doi.org/10.1023/A:1009870521175

6. Percy DM, Argus GW, Cronk QC, Fazekas AJ, Kesanakurti PR, Burgess KS, Husband BC, Newmaster SG, Barrett SCH, Graham SW (2014) Understanding the spectacular failure of DNA barcoding in willows (*Salix*): Does this result from a trans-specific selective sweep? Mol Ecol 23:4737-4756. https://doi.org/10.1111/mec.12837

7. Hardig TM, Brunsfeld SJ, Fritz RS, Morgan M, Orians CM (2000) Morphological and molecular evidence for hybridization and introgression in a willow (*Salix*) hybrid zone. Mol Ecol 9:9-24. https://doi.org/10.1046/j.1365-294X.2000.00757.x

8. Lin J, Gibbs JP, Smart LB (2009) Population genetic structure of native versus naturalized sympatric shrub willows (*Salix*: Salicaceae). Am J Bot 96:771-785. https://doi.org/10.3732/ajb.0800321

9. Heribert-Nilsson N (1918) Experimentelle studien uber variabiliät, Spaltung, Artibildung, und evoluation in der gattung *Salix*. Lunds Universitats Arsskrift N. F. Avd 2.

10. Karp A, Hanley S, Trybush S, Macalpine W, Pei MH, Shield I (2011) Genetic improvement of willow for bioenergy and biofuels. J Integ Plant Biol 53. https://doi.org/10.1111/j.1744-7909.2010.01015.x

11. Kuzovkina YA, Weih M, Romero MA, Charles J, Hust S, McIvor I, Karp A, Trybush S, Labrecque M, Teodorescu TI, Singh NB, Smart LB, Volk TA (2008) *Salix*: Botany and Global Horticulture. Horticultural Reviews. John Wiley & Sons, Inc., pp 447-489. https://doi.org/10.1002/9780470380147.ch8

12. Birchler JA, Yao H, Chudalayandi S (2006) Unraveling the genetic basis of hybrid vigor. Proc Natl Acad Sci U S A 103:12957-12958. https://doi.org/10.1073/pnas.0605627103

13. Soltis DE, Albert VA, Leebens-Mack J, Bell CD, Paterson AH, Zheng C, Sankoff D, dePamphilis CW, Wall PK, Soltis PS (2009) Polyploidy and angiosperm diversification. Am J Bot 96:336-348. https://doi.org/10.3732/ajb.0800079

14. Wagner ND, He L, Hörandl E (2020) Phylogenomic relationships and evolution of polyploid *Salix* species revealed by RAD sequencing data. Front Plant Sci 11:1077. https://doi.org/10.3389/fpls.2020.01077

15. Chen ZJ (2010) Molecular mechanisms of polyploidy and hybrid vigor. Trends Plant Sci 15:57-71. https://doi.org/10.1016/j.tplants.2009.12.003

16. Volk TA, Abrahamson LP, Cameron KD, Castellano P, Corbin T, Fabio E, Johnson G, Kuzovkina-Eischen Y, Labrecque M, Miller R, Sidders D, Smart LB, Staver K, Stanosz GR, Rees Kv (2011) Yields of willow biomass crops across a range of sites in North America. Asp Appl Biol 112:67-74

17. Fabio ES, Volk TA, Miller RO, Serapiglia MJ, Kemanian AR, Montes F, Kuzovkina YA, Kling GJ, Smart LB (2017) Contributions of environment and genotype to variation in shrub willow biomass composition. Ind Crop Prod 108:149-161. https://doi.org/10.1016/j.indcrop.2017.06.030

18. Zsuffa L, Mosseler A, Raj Y (1984) Prospects for interspecific hybridization in willow for biomass production. In: Perttu KL (ed) Ecology and Management of Forest Biomass

534 Production Systems. Report 15: Swedish University of Agricultural Sciences, Uppsala,
535 Sweden.

536 19. Orians CM (2000) The effects of hybridization in plants on secondary chemistry:
537 implications for the ecology and evolution of plant–herbivore interactions. Am J Bot 87:1749-
538 1756. https://doi.org/10.2307/2656824

539 20. Hallgren P, Ikonen A, Hjältén J, Roininen H (2003) Inheritance patterns of phenolics in F1,
540 F2, and backcross hybrids of willows: Implications for herbivore responses to hybrid plants. J
541 Chem Ecol 29:1143-1158. https://doi.org/10.1023/A:1023829506473

542 21. Wang W, Carlson CH, Smart LB, Carlson JE (2020) Transcriptome analysis of contrasting
543 resistance to herbivory by *Empoasca fabae* in two shrub willow species and their hybrid
544 progeny. PLoS ONE 15:e0236586. https://doi.org/10.1371/journal.pone.0236586

545 22. Johansson LKH, Alstrom S (2000) Field resistance to willow leaf rust *Melampsora epitea* in
546 inter- and intraspecific hybrids of *Salix viminalis* and *S. dasyclados*. Eur J Plant Pathol
547 106:763-769. https://doi.org/10.1023/a:1026573219481

548 23. Orians CM, Huang CH, Wild A, Dorfman KA, Zee P, Dao MTT, Fritz RS (1997) Willow
549 hybridization differentially affects preference and performance of herbivorous beetles.
550 Entomol Expr Appl 83:285-294. https://doi.org/10.1046/j.1570-7458.1997.00183.x

551 24. Orians CM, Griffiths ME, Roche BM, Fritz RS (2000) Phenolic glycosides and condensed
552 tannins in *Salix sericea*, *S. eriocephala* and their F1 hybrids: not all hybrids are created equal.
553 Biochem Syst Ecol 28:619-632. https://doi.org/10.1016/S0305-1978(99)00101-5

554 25. Orians CM, Fritz RS, Hochwender CG, Albrectsen BR, Czesak ME (2013) How slug
555 herbivory of juvenile hybrid willows alters chemistry, growth and subsequent susceptibility to
556 diverse plant enemies. Ann Bot 112:757-765. https://doi.org/10.1093/aob/mct002

557 26. Cameron KD, Phillips IS, Kopp RF, Volk TA, Maynard CA, Abrahamson LP, Smart LB
558 (2008) Quantitative genetics of traits indicative of biomass production and heterosis in 34
559 full-sib F_1 *Salix eriocephala* families. Bioenerg Res 1:80-90. https://doi.org/10.1007/s12155-
560 008-9006-x

561 27. Fabio ES, Kemanian AR, Montes F, Miller RO, Smart LB (2017) A mixed model approach
562 for evaluating yield improvements in interspecific hybrids of shrub willow, a dedicated
563 bioenergy crop. Ind Crop Prod 96:57-70. https://doi.org/10.1016/j.indcrop.2016.11.019

564 28. Nilsson-Ehle H (1936) A gigasform found in nature from *Populus tremula*. Hereditas
565 21:379-382.

566 29. Fabio ES, Volk TA, Miller RO, Serapiglia MJ, Gauch HG, Van Rees KC, Hangs RD,
567 Amichev BY, Kuzovkina YA, Labrecque M (2016) Genotype by environment interactions
568 analysis of North American shrub willow yield trials confirms superior performance of
569 triploid hybrids. GCB Bioenergy 9:445-459. https://doi.org/10.1111/gcbb.12344

570 30. Serapiglia MJ, Gouker FE, Smart LB (2014) Early selection of novel triploid hybrids of
571 shrub willow with improved biomass yield relative to diploids. BMC Plant Biol 14:74.
572 https://doi.org/10.1186/1471-2229-14-74

573 31. Carlson CH, Gouker FE, Crowell CR, Evans L, DiFazio SP, Smart CD, Smart LB (2019)
574 Joint linkage and association mapping of complex traits in shrub willow (*Salix purpurea* L.).
575 Ann Bot 124:701-716. https://doi.org/10.1093/aob/mcz047

576 32. Carlson CH, Smart LB (2016) Electrical capacitance as a predictor of root dry weight in
577 shrub willow (*Salix*; Salicaceae) parents and progeny. Appl Plant Sci 4:e1600031.
578 https://doi.org/10.3732/apps.1600031

579 33. R Core Team (2017) R: A language and environment for statistical computing. R Foundation
580 for Statistical Computing, Vienna, Australia.

581 34. Bates D, Mächler M, Bolker B, Walker S (2015) Fitting linear mixed-effects models using
582 lme4. J Stat Soft 67:48. https://doi.org/10.18637/jss.v067.i01

583 35. Velazco JG, Rodriguez-Alvarez MX, Boer MP, Jordan DR, Eilers PHC, Malosetti M, van
584 Eeuwijk FA (2017) Modelling spatial trends in sorghum breeding field trials using a two-
585 dimensional P-spline mixed model. Theor Appl Genet 130:1375-1392.
586 https://doi.org/10.1007/s00122-017-2894-4

587 36. Rodríguez-Álvarez MX, Lee D-J, Kneib T, Durbán M, Eilers P (2015) Fast smoothing
588 parameter separation in multidimensional generalized P-splines: the SAP algorithm. Stat
589 Comp 25:941-957. https://doi.org/10.1007/s11222-014-9464-2

590 37. Faliński JB (1980) Vegetation dynamics and sex structure of the populations of pioneer
591 dioecious woody plants. Vegetatio 43:23-38. https://doi.org/10.1007/BF00121014

592 38. Crawford R, Balfour J (1983) Female predominant sex ratios and physiological
593 differentiation in arctic willows. J Ecol 71:149-160. https://doi.org/10.2307/2259968

594 39. Alliende M, Harper J (1989) Demographic studies of a dioecious tree. I. Colonization, sex
595 and age structure of a population of *Salix cinerea*. J Ecol 77:1029-1047.
596 https://doi.org/10.2307/2260821

597 40. Dawson TE, Bliss L (1989) Patterns of water use and the tissue water relations in the
598 dioecious shrub, *Salix arctica*: the physiological basis for habitat partitioning between the
599 sexes. Oecologia 79:332-343. https://doi.org/10.1007/BF00384312

600 41. Alström-Rapaport C, Lascoux M, Gullberg U (1997) Sex determination and sex ratio in the
601 dioecious shrub *Salix viminalis* L. Theor Appl Genet 94:493-497.
602 https://doi.org/10.1007/s001220050442

603 42. Ueno N, Suyama Y, Seiwa K (2007) What makes the sex ratio female-biased in the dioecious
604 tree *Salix sachalinensis*? J Ecol 95:951-959. https://doi.org/10.1111/j.1365-
605 2745.2007.01269.x

606 43. Che-Castaldo C, Crisafulli CM, Bishop JG, Fagan WF (2015) What causes female bias in the
607 secondary sex ratios of the dioecious woody shrub *Salix sitchensis* colonizing a primary
608 successional landscape? Am J Bot 102 (8):1309-1322. https://doi.org/10.3732/ajb.1500143

609 44. Yin T, DiFazio SP, Gunter LE, Zhang X, Sewell MM, Woolbright SA, Allan GJ, Kelleher
610 CT, Douglas CJ, Wang M, Tuskan GA (2008) Genome structure and emerging evidence of an
611 incipient sex chromosome in *Populus*. Genome Res 18:422-430.
612 https://doi.org/10.1101/gr.7076308

613 45. Fabio ES, Smart LB (2018) Effects of nitrogen fertilization in shrub willow short rotation
614 coppice production - a quantitative review. GCB Bioenergy 10:548-564.
615 https://doi.org/10.1111/gcbb.12507

616

Tables

Table 1. Description of intra- and interspecific shrub willow family parents, pedigree, ploidy-level, total number of progeny (N) included in the trial. Chi-square (χ^2) to test the null hypothesis of a 1:1 sex ratio (F = female, M = male).

Family	Female	Male	Pedigree[1]	Ploidy	N	F	M	F:M	χ^2
82	94006	94001	*S. pur* × *S. pur*	2*x*	100	71	29	2.44	46.2***
317	Wolcott	Fish Creek	*S. pur* × *S. pur*	2*x*	482	266	216	1.23	5.19*
407	94006	Jorr	*S. pur* × *S. vim*	2*x*	100	60	40	1.50	4.00*
421	07-MBG-5027	94001	*S. vim* × *S. pur*	2*x*	100	53	47	1.13	0.36^{ns}
415	94006	01-200-003	*S. pur* × *S. miy*	3*x*	100	56	44	1.27	1.44^{ns}
423	07-MBG-5027	01-200-003	*S. vim* × *S. miy*	3*x*	63	36	27	1.33	1.26^{ns}
430	01-200-006	Jorr	*S. miy* × *S. vim*	3*x*	23	23	0	*inf*	23.0***
425	01-200-006	SX64	*S. miy* × *S. miy*	4*x*	100	82	18	4.56	40.9***

[1]*Salix purpurea* (*S. pur*), *Salix viminalis* (*S. vim*), and *Salix miyabeana* (*S. miy*).

$^{*}P < 0.05$, $^{**}P < 0.01$, $^{***}P < 0.001$; ns = non-significant

641 **Table 2.** Trait descriptions, abbreviations, and units, and time of measurement in years post-coppice (Yr)
642 for field traits, and days after planting (dap) for greenhouse traits.

Abbreviation	Trait	Units	Field (Yr)	Greenhouse (dap)
Biomass				
SDW	Total stem dry weight	g	-	77
LDW	Total leaf dry weight	g	-	77
RDW	Total root dry weight	g	-	77
Stem measurements				
HT	Plot height	m	0, 1, 2	14-77
TSL	Total stem length	cm	-	14-77
MSL	Mean stem length	cm	-	14-77
STN	Stem number	#	0, 1, 2	14-77
DIA	Stem diameter	mm	1, 2	77
SA	Stem area	cm^2	1, 2	77
VOL	Stem volume	cm^3	1, 2	77
DVOL	Stem mass	g	1, 2	77
ASN	Axial stem number	#	-	35, 70
Foliar measurements				
LFA	Leaf area	cm^2	1, 2	70
LFL	Leaf length	cm	1, 2	70
LFW	Leaf width	cm	1, 2	70
LFP	Leaf perimeter	cm	1, 2	70
LFF	Leaf shape factor	0-1	1, 2	70
LFR	Leaf aspect ratio	-	1, 2	70
LFDW	Leaf dry weight	g	1, 2	70
SLA	Specific leaf area	$cm^2\ g^{-1}$	1, 2	70
Canopy Architecture				
CDIA	Crown diameter	cm	0, 1, 2	-
FORM	Crown form	°	0, 1, 2	-
Wood Chemical Composition				
HCL	Hemicellulose content	%	2	-
CLS	Cellulose content	%	2	-
LIG	Lignin content	%	2	-
ASH	Ash content	%	2	-
DEN	Wood density	$g\ cm^{-3}$	1, 2	-
Physiology and Phenology				
SPAD	SPAD	-	0, 1, 2	14, 42, 70
RGR	Relative growth rate	$cm\ d^{-1}$	0, 1.1, 1.2, 2	14-77
REC	Root electrical capacitance	nF	-	77
STC	Stem color	(0, 1, 2)	0	-
PHE	Vegetative phenology	0-5	-	7, 9, 11, 13, 15

643

644

645

646

647

Figure Captions

Figure 1. Harvested dry biomass by family, genotype, and ploidy. Overlain **(a)** barplots of mean (±SE) SDW, LDW, and RDW biomass by family. For each trait, letters above bars represent significant differences by family according to Tukey's HSD groupings ($\alpha = 0.05$). The **(b)** aboveground biomass means (±SE) all parent and progeny genotypes (n = 104) are shown in descending order. Bars are filled according to the ploidy of each genotype and filled circles below bars specify the location of the parents. Boxplot distributions depict the median and interquartile range (IQR ±1.5) of **(c)** biomass dry wt. **(d)** and biomass dry wt. ratios by ploidy, where asterisks denote significant differences at a Wilcoxon $P < 0.05$*, < 0.01**, and < 0.001***.

Figure 2. Total aboveground dry biomass means of triploid families and respective female (P1) and male (P2) parents. Bars are colored according to ploidy-level (see legend). Asterisks *** above bars denote significant differences ($P < 0.001$).

Figure 3. Repeated physiological measurements by ploidy. Boxplot distributions depict the median and interquartile range (IQR ±1.5) of **(a)** phenological stages (PHE) at 7, 9, 11, and 13 days after planting (dap) as well as **(b)** SPAD values by ploidy. Asterisks above or below boxplots of diploids (beige), triploids (cyan), and tetraploids (dark grey) denote significant differences at a Wilcoxon $P < 0.05$*, < 0.01**, and < 0.001***. The 15 dap stage is not shown because there were no significant differences by ploidy.

Figure 4. Midparent heterosis (MPH %) for greenhouse collected traits in triploids and tetraploids. Boxplot distributions are shown as the percent deviation of the hybrid from the midparent and depict the median and interquartile range (IQR ±1.5) of MPH for each trait by family, which are filled according to the legend above panels.

Figure 5. Inheritance patterns growth traits among hybrid shrub willow families. Each point represents a single trait plotted as the $\log_2$ difference of the progeny from the female ($\log_2 (F_1/P1)$, horizontal axis) and male ($\log_2 (F_1/P2)$, vertical axis) parents. Stem traits are characterized by filled black points and foliar traits, by filled white points. Red lines passing through each point represents the corresponding ± standard error of the family mean.

Figure 6. Midparent heterosis (MPH %) for field collected traits in triploids and tetraploids. Boxplot distributions are shown as the percent deviation of the hybrid from the midparent and depict the median and interquartile range (IQR ±1.5) of MPH for each trait by family, which are filled according to the legend above panels.

Fig. 1

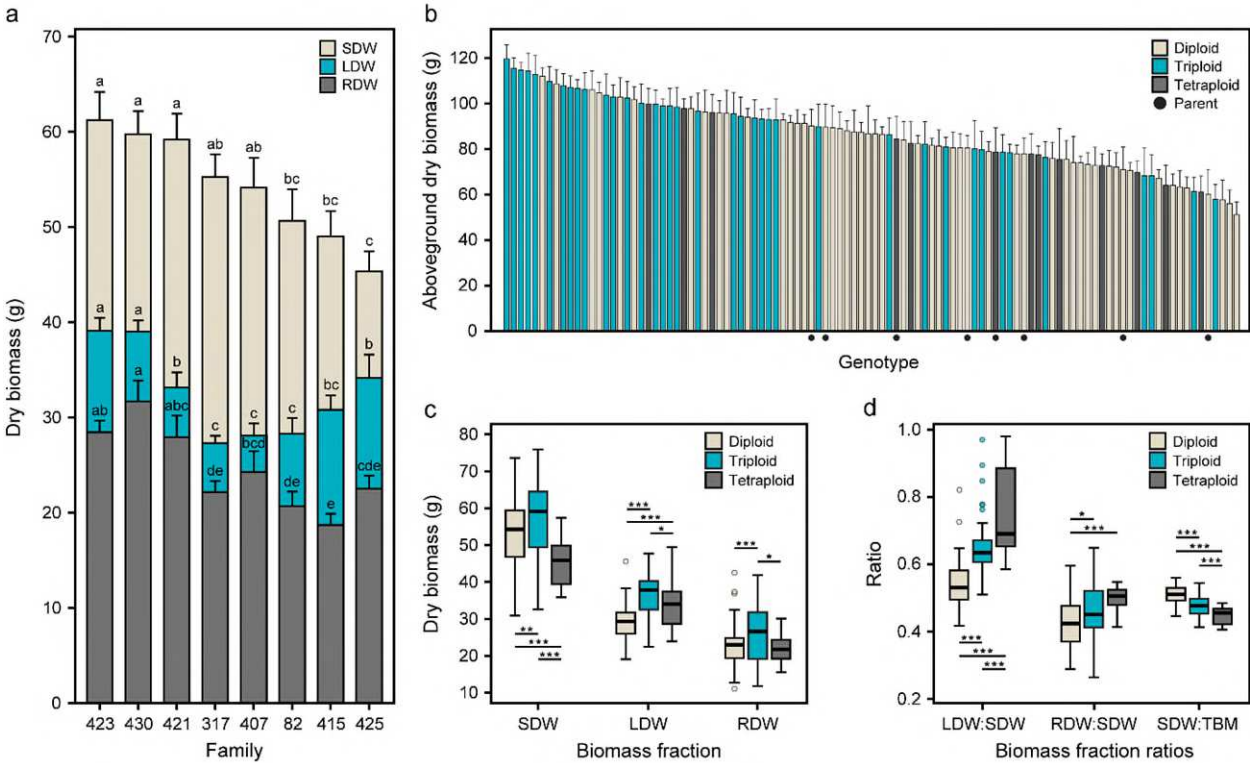
a
Dry biomass (g)
SDW
LDW
RDW
423 430 421 317 407 82 415 425
Family
b
Aboveground dry biomass (g)
Diploid
Triploid
Tetraploid
Parent
Genotype
c
Dry biomass (g)
Diploid
Triploid
Tetraploid
SDW
LDW
RDW
Biomass fraction
d
Ratio
Diploid
Triploid
Tetraploid
LDW:SDW
RDW:SDW
SDW:TBM
Biomass fraction ratios

Fig. 2

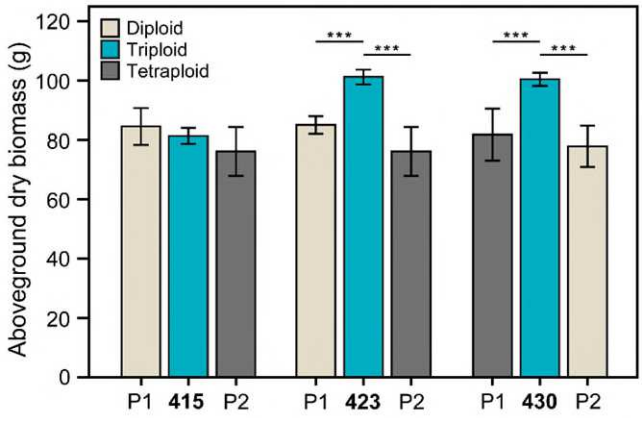
Diploid
Triploid
Tetraploid
Aboveground dry biomass (g)
120
100
80
60
40
20
0
***
***
***
***
P1
415
P2
P1
423
P2
P1
430
P2

Fig. 3

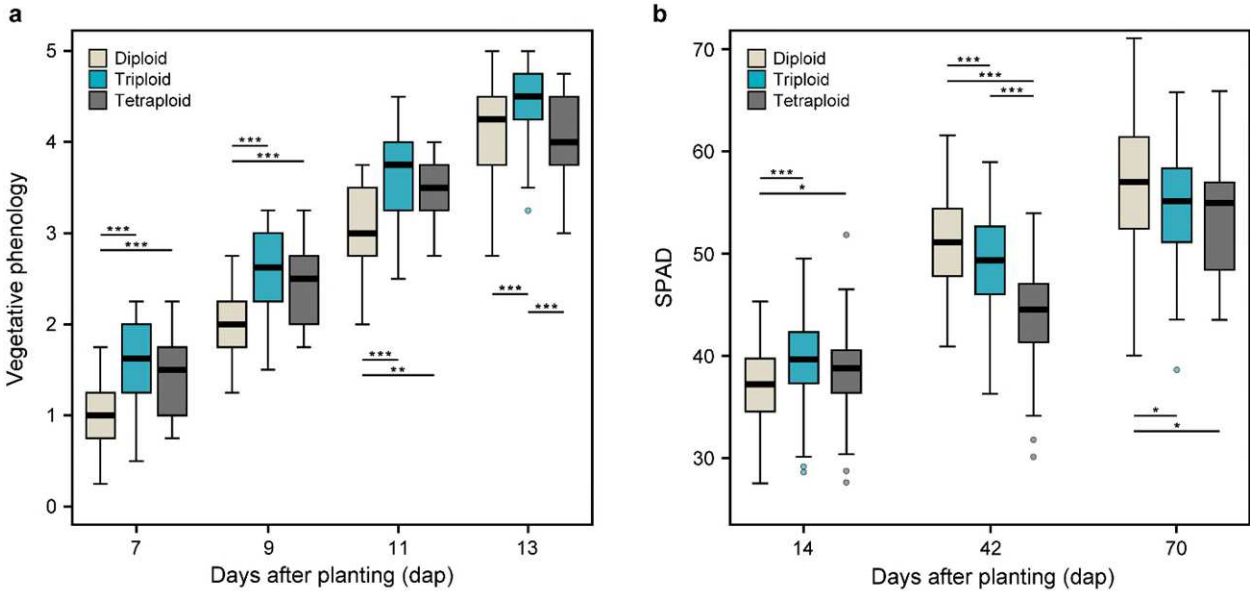
a
Diploid
Triploid
Tetraploid
Vegetative phenology
Days after planting (dap)
b
SPAD
Days after planting (dap)

726 **Fig. 4**

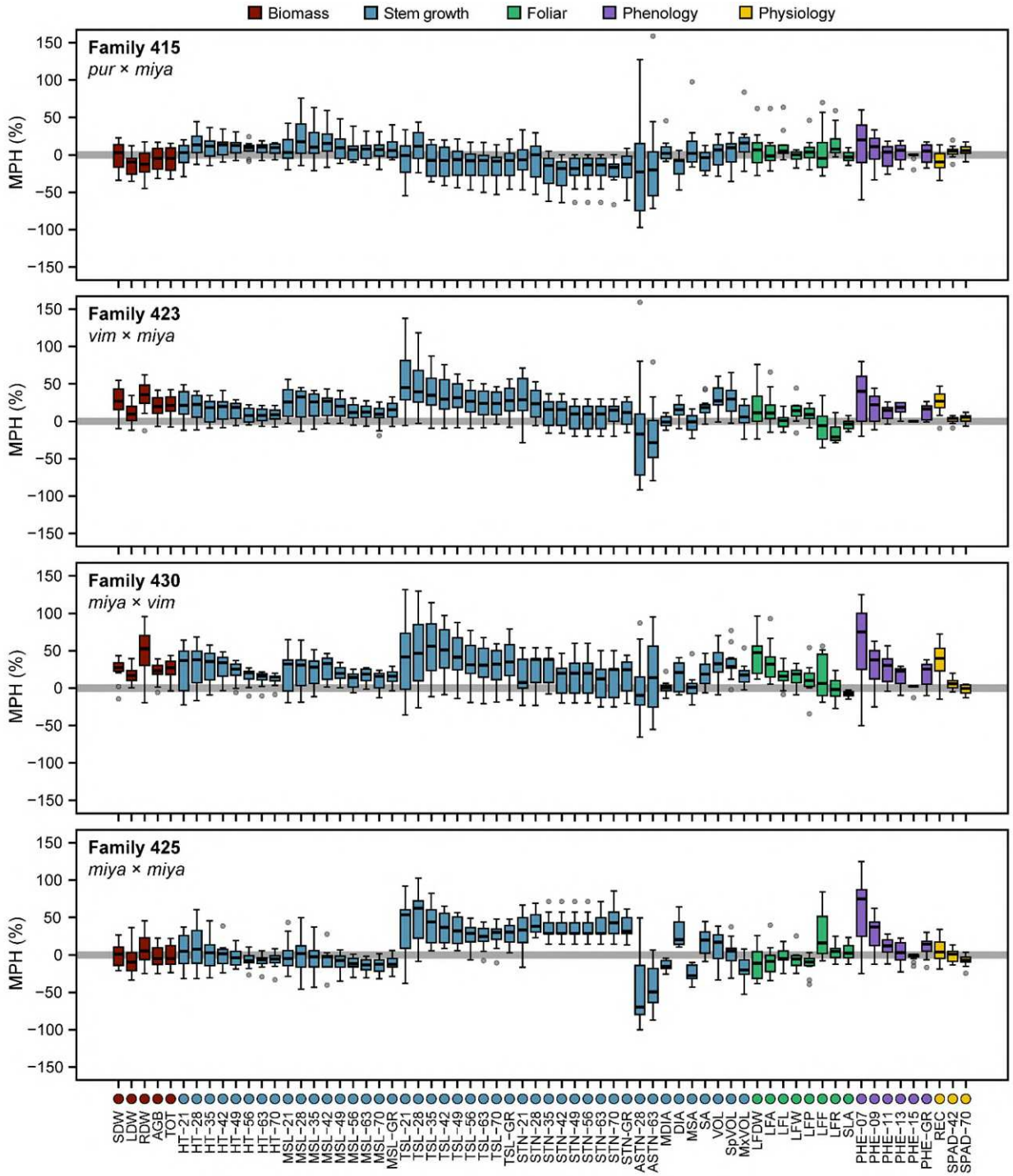

727

728

729

730

731

Fig. 5

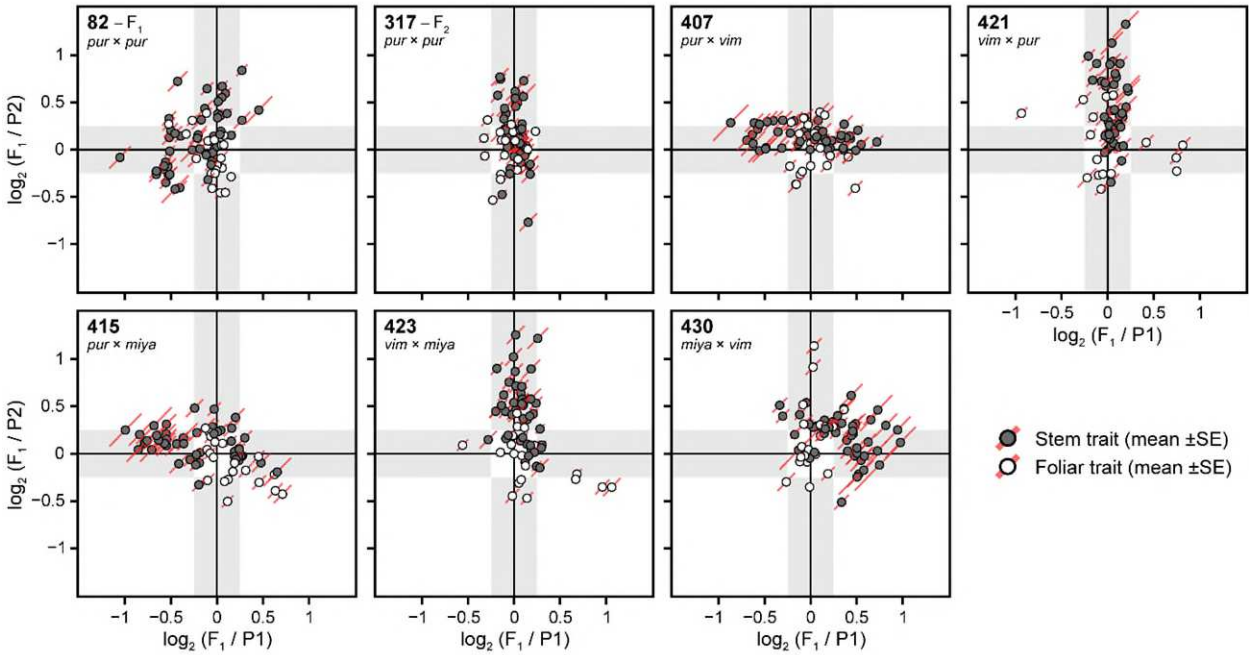
82 – F1
pur × pur
317 – F2
pur × pur
407
pur × vim
421
vim × pur
415
pur × miya
423
vim × miya
430
miya × vim
log2 (F1 / P2)
log2 (F1 / P1)
Stem trait (mean ±SE)
Foliar trait (mean ±SE)

751 **Fig. 6**

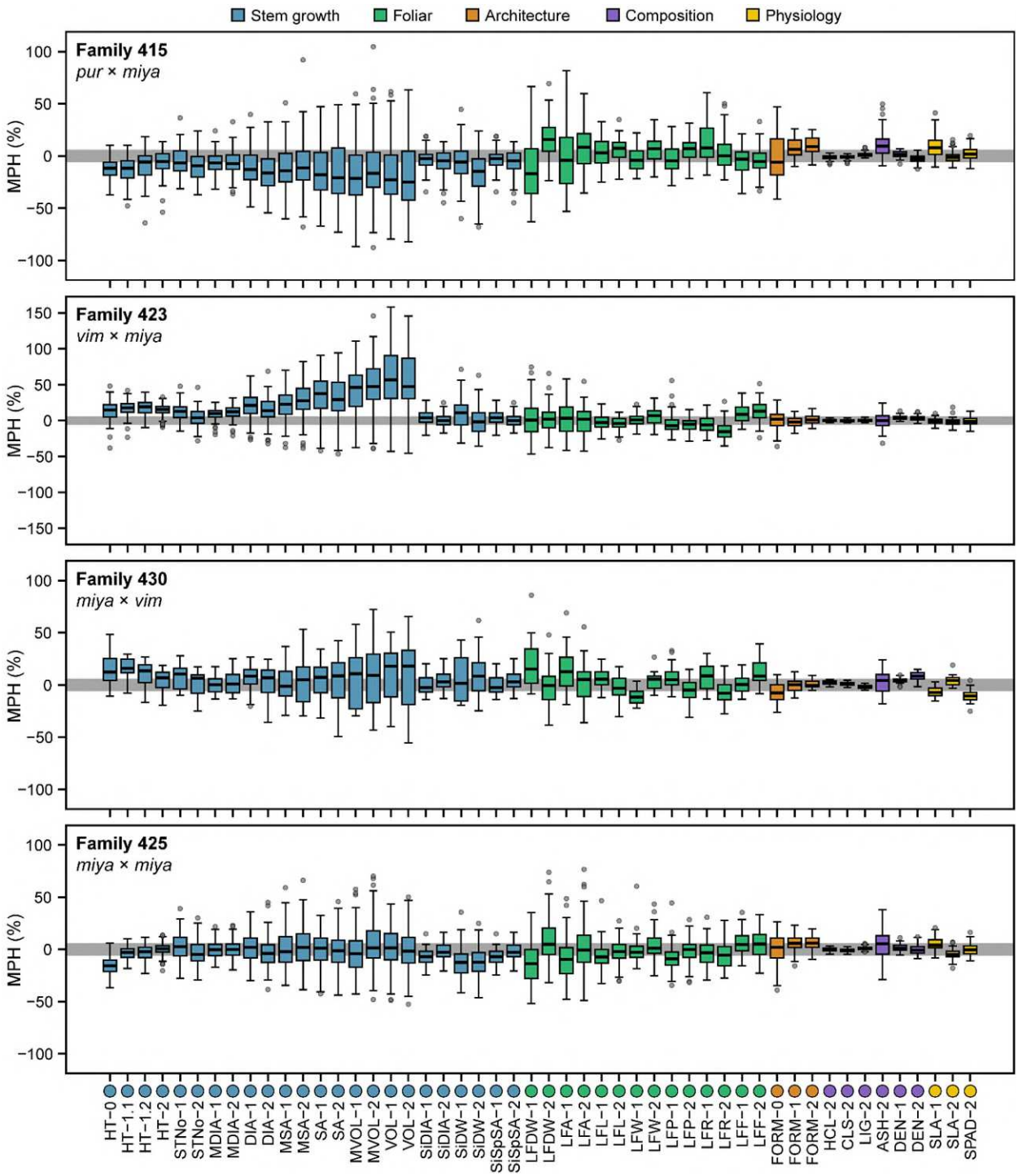

752

753

754

755

Supplementary Material

Supplementary Figure S1. Aerial image of the field trial located at Cornell AgriTech (Geneva, NY).

Supplementary Figure S2. Midparent heterosis (MPH %) for greenhouse collected traits in diploids. Boxplot distributions are shown as the percent deviation of the hybrid from the midparent and depict the median and interquartile range (IQR ±1.5) of MPH for each trait by family, which are filled according to the legend above panels.

Supplementary Figure S3. Pairwise correlations of biomass traits collected in the greenhouse. The correlation matrix was re-ordered by hierarchical clustering using the *average* distance method. Beneath trait abbreviations in the first row and in the final column, filled-circles highlight major trait classes detailed in the legend. Increasing in intensity with higher absolute Pearson correlation coefficients (r), positive correlations are illustrated by filled blue squares and negative correlations by filled-red squares. Non-significant correlations ($P > 0.01$) were left blank. Significance levels were used to scale the area of each square, such that smaller squares represent correlations with lower significance and larger squares represent those showing more significance.

Supplementary Figure S4. Pairwise correlations of biomass traits collected in the field. The correlation matrix was re-ordered by hierarchical clustering using the *average* distance method. Beneath trait abbreviations in the first row and in the final column, filled-circles highlight major trait classes detailed in the legend. Increasing in intensity with higher absolute Pearson correlation coefficients (r), positive correlations are illustrated by filled blue squares and negative correlations by filled-red squares. Non-significant correlations ($P > 0.01$) were left blank. Significance levels were used to scale the area of each square, such that smaller squares represent correlations with lower significance and larger squares represent those showing more significance.

Supplementary Figure S5. Wood chemical composition associations from second year post-coppice measurements. Points within each scatterplot are colored according to individual ploidy-level, according to the legend above figure panels.

Supplementary Figure S6. Midparent heterosis (MPH %) for field collected traits in diploids. Boxplot distributions are shown as the percent deviation of the hybrid from the midparent and depict the median and interquartile range (IQR ±1.5) of MPH for each trait by family, which are filled according to the legend above panels.

Figures

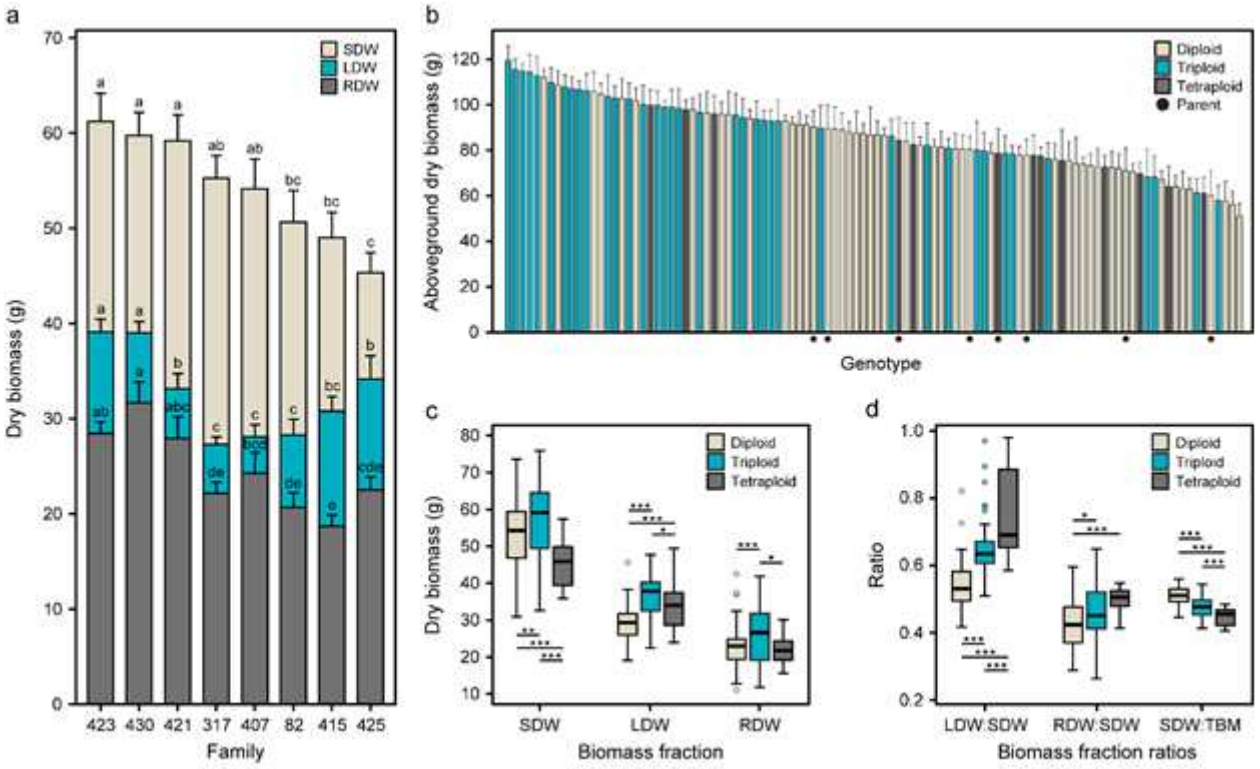

Figure 1

Harvested dry biomass by family, genotype, and ploidy. Overlain (a) barplots of mean (±SE) SDW, LDW, and RDW biomass by family. For each trait, letters above bars represent significant differences by family according to Tukey's HSD groupings (α = 0.05). The (b) aboveground biomass means (±SE) all parent and progeny genotypes (n = 104) are shown in descending order. Bars are filled according to the ploidy of each genotype and filled circles below bars specify the location of the parents. Boxplot distributions depict the median and interquartile range (IQR ±1.5) of (c) biomass dry wt. (d) and biomass dry wt. ratios by ploidy, where asterisks denote significant differences at a Wilcoxon P < 0.05*, < 0.01**, and < 0.001***.

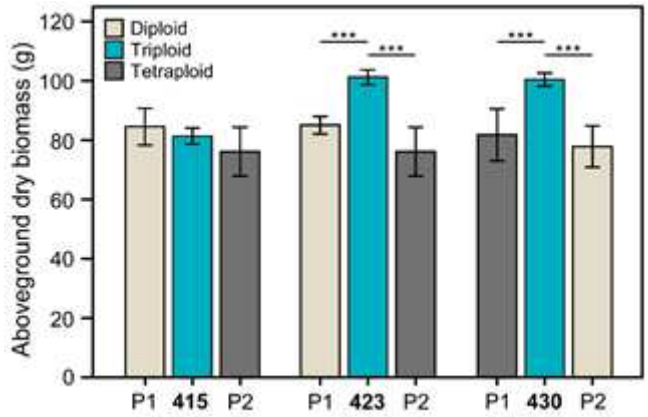

Figure 2

Total aboveground dry biomass means of triploid families and respective female (P1) and male (P2) parents. Bars are colored according to ploidy-level (see legend). Asterisks *** above bars denote significant differences (P < 0.001).

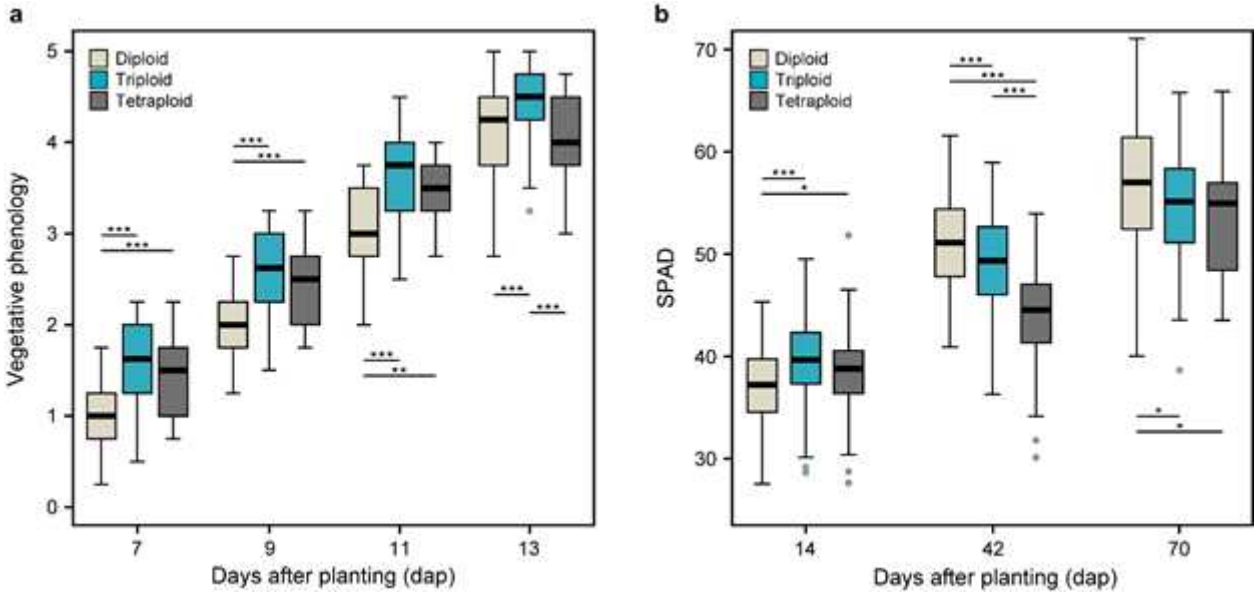

Figure 3

Repeated physiological measurements by ploidy. Boxplot distributions depict the median and interquartile range (IQR ±1.5) of (a) phenological stages (PHE) at 7, 9, 11, and 13 days after planting (dap) as well as (b) SPAD values by ploidy. Asterisks above or below boxplots of diploids (beige), triploids (cyan), and tetraploids (dark grey) denote significant differences at a Wilcoxon P < 0.05*, < 0.01**, and < 0.001***. The 15 dap stage is not shown because there were no significant differences by ploidy.

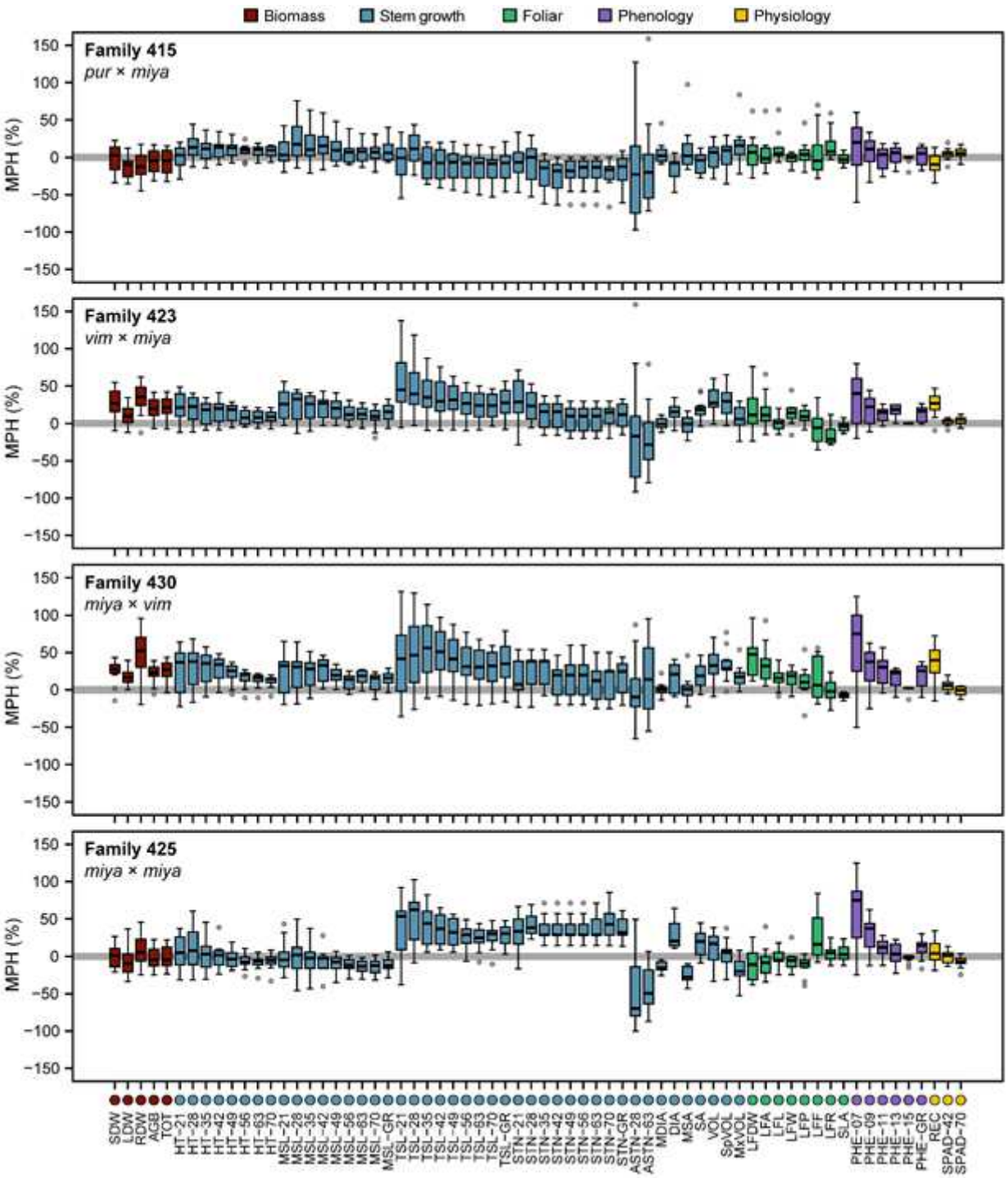

Figure 4

Midparent heterosis (MPH %) for greenhouse collected traits in triploids and tetraploids. Boxplot distributions are shown as the percent deviation of the hybrid from the midparent and depict the median and interquartile range (IQR ±1.5) of MPH for each trait by family, which are filled according to the legend above panels.

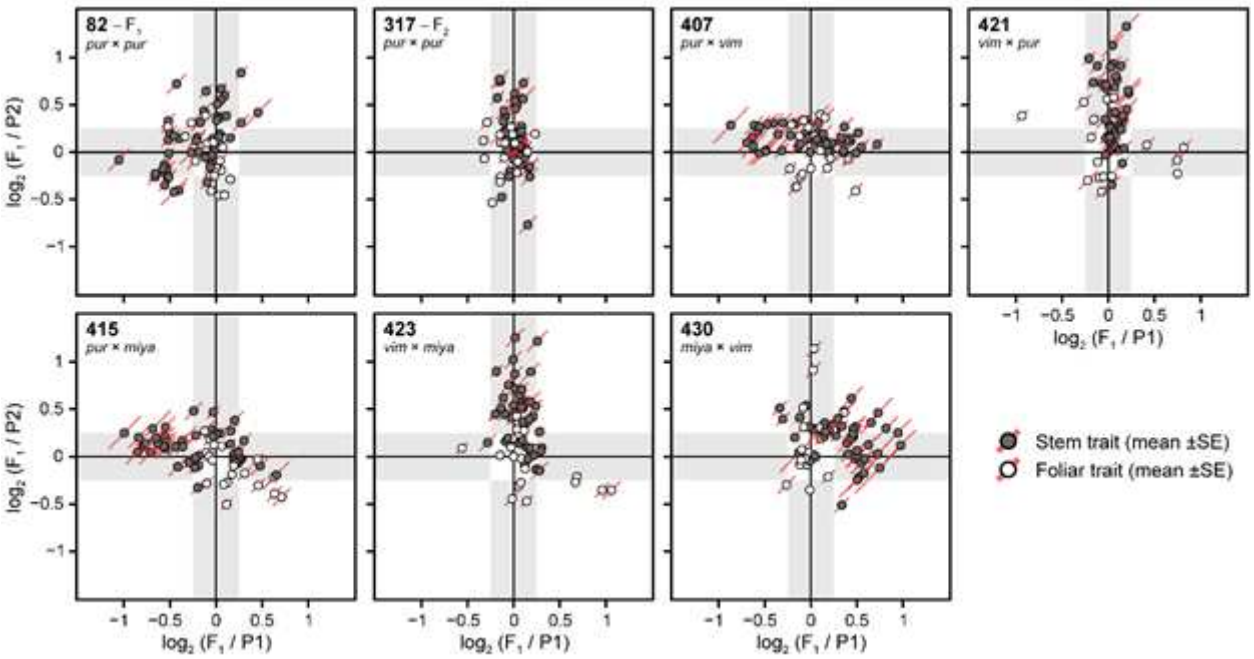

Figure 5

Inheritance patterns growth traits among hybrid shrub willow families. Each point represents a single trait plotted as the log2 difference of the progeny from the female (log2 (F1/P1), horizontal axis) and male (log2 (F1/P2), vertical axis) parents. Stem traits are characterized by filled black points and foliar traits, by filled white points. Red lines passing through each point represents the corresponding ± standard error of the family mean.

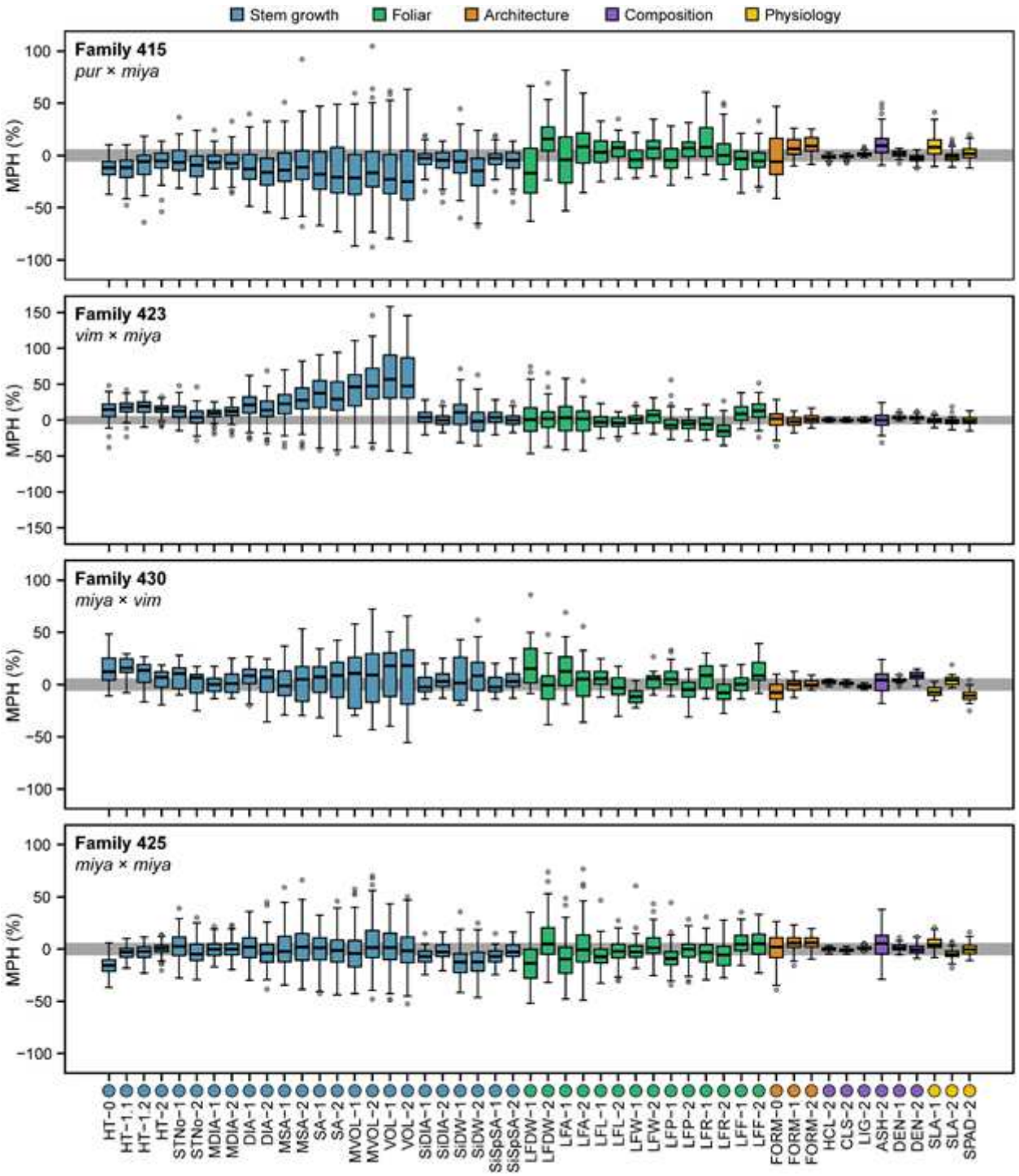

Figure 6

Midparent heterosis (MPH %) for field collected traits in triploids and tetraploids. Boxplot distributions are shown as the percent deviation of the hybrid from the midparent and depict the median and interquartile range (IQR ±1.5) of MPH for each trait by family, which are filled according to the legend above panels.

Supplementary Files

This is a list of supplementary files associated with this preprint. Click to download.

- CarlsonandSmartTriploidheterosisSupplementaryMaterial.pdf